Article

Cell Reports

Noncanonical Genomic Imprinting Effects in Offspring

Graphical Abstract

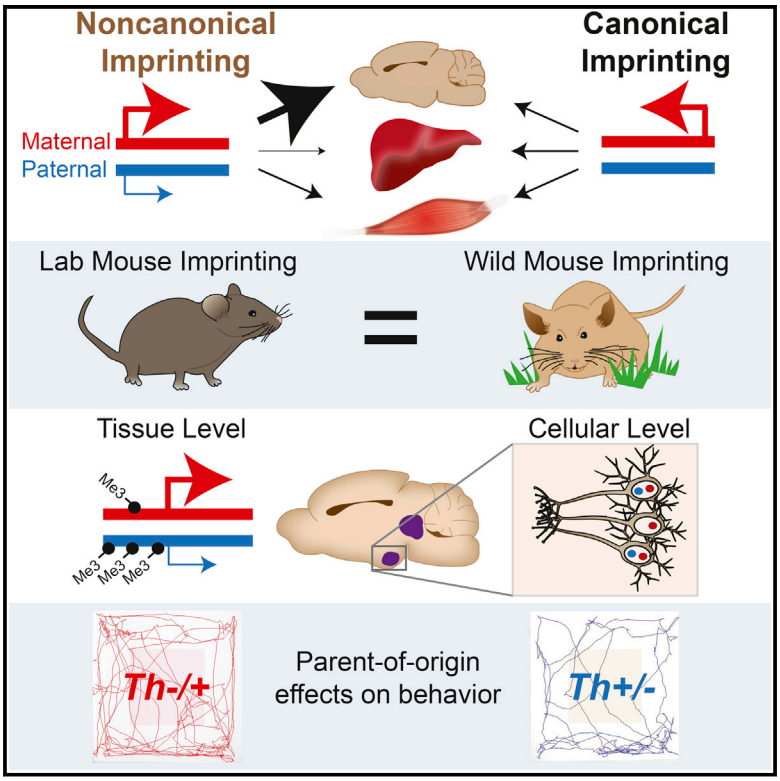

Authors

Paul J. Bonthuis, Wei-Chao Huang, Cornelia N. Stacher Hörndli, Elliott Ferris, Tong Cheng, Christopher Gregg

Correspondence

chris.gregg@neuro.utah.edu

In Brief

Canonical imprinting involves silencing of the maternal or paternal allele. Bonthuis et al. describe tissue-specific noncanonical imprinting effects involving maternal or paternal allele expression biases. Noncanonical imprinted genes are enriched in the brain and, at the cellular level, exhibit allele-specific expression effects in discrete subpopulations of neurons. They find that noncanonical imprinting can lead to parent-of-origin effects for inherited mutations that impact brain function and behavior.

Highlights

- Sensitive RNA-seq approach detects tissue-specific maternal and paternal allele biases
- Noncanonical imprinting effects are conserved in wild populations
- Nascent RNA in situ hybridization reveals allelic effects in subpopulations of neurons
- Noncanonical imprinting influences the monoamine pathway and offspring behavior

Accession Numbers

GSE70484

Bonthuis et al., 2015, Cell Reports *12*, 979–991
August 11, 2015
http://dx.doi.org/10.1016/j.celrep.2015.07.017

Cell Reports
Article

Noncanonical Genomic Imprinting Effects in Offspring

Paul J. Bonthuis,[1,3] Wei-Chao Huang,[1,3] Cornelia N. Stacher Hörndli,[1,3] Elliott Ferris,[1,3] Tong Cheng,[1,3] and Christopher Gregg[1,2,*]
[1]Department of Neurobiology & Anatomy
[2]Department of Human Genetics
University of Utah School of Medicine, Salt Lake City, UT 84132-3401, USA
[3]Co-first author
*Correspondence: chris.gregg@neuro.utah.edu
http://dx.doi.org/10.1016/j.celrep.2015.07.017

SUMMARY

Here, we describe an RNA-sequencing (RNA-seq)-based approach that accurately detects even modest maternal or paternal allele expression biases at the tissue level, which we call noncanonical genomic imprinting effects. We profile imprinting in the arcuate nucleus (ARN) and dorsal raphe nucleus of the female mouse brain as well as skeletal muscle (mesodermal) and liver (endodermal). Our study uncovers hundreds of noncanonical autosomal and X-linked imprinting effects. Noncanonical imprinting is highly tissue-specific and enriched in the ARN, but rare in the liver. These effects are reproducible across different genetic backgrounds and associated with allele-specific chromatin. Using in situ hybridization for nascent RNAs, we discover that autosomal noncanonical imprinted genes with a tissue-level allele bias exhibit allele-specific expression effects in subpopulations of neurons in the brain in vivo. We define noncanonical imprinted genes that regulate monoamine signaling and determine that these effects influence the impact of inherited mutations on offspring behavior.

INTRODUCTION

Many inherited genetic risk factors for complex disorders, such as neuropsychiatric disorders, are heterozygous in the affected individuals (Huguet et al., 2013). Therefore, understanding allele-specific expression effects in different tissues and cell types is essential for understanding how inherited mutations may impact offspring. Genomic imprinting is a heritable form of epigenetic gene regulation that results in preferential expression of the maternal or paternal allele for at least 100 genes in mammals (Bartolomei and Ferguson-Smith, 2011). In females, imprinting can influence both autosomal and X-linked genes, and a consequence of imprinting is that the effect of an inherited mutation is influenced by the parental origin.

Canonical imprinting is associated with complete silencing of one gene copy. Indeed, models of the Kinship Theory for the evolution of imprinting predict that evolutionary parental conflicts drive complete silencing of one parent's allele at loci that influence offspring demands on maternal resources (Haig, 2000). However, early studies noted that some imprinted genes exhibit a bias to express either the maternal or paternal allele, rather than complete silencing (Khatib, 2007). Compared to canonical imprinted genes, genes that exhibit allele expression biases might be associated with different mechanisms, functions, and selective pressures. Here, we refer to these effects as "noncanonical imprinting effects." Previously, we devised an approach to profile imprinting in the developing and adult mouse brain using RNA sequencing (RNA-seq) (Gregg et al., 2010a, 2010b) and uncovered noncanonical imprinting effects that influence the expression of hundreds of genes. On the other hand, some other studies of imprinting in somatic tissues found very few novel imprinted genes in mice (Babak et al., 2008; Wang et al., 2008), whereas a study of the mouse liver uncovered 535 imprinted genes (Goncalves et al., 2012). Our findings have been debated (DeVeale et al., 2012), and two recent studies of imprinting in different mouse tissues reached different conclusions regarding the prevalence of imprinting and the identity of the novel imprinted genes detected (Babak et al., 2015; Crowley et al., 2015). Thus, noncanonical imprinting effects in the genome remain poorly understood, and the mechanisms involved and possible function(s) of noncanonical imprinting are unknown.

Here, we devise and apply improved methods to detect imprinting in different tissues by RNA-seq. We perform a genome-wide analysis of canonical and noncanonical imprinting effects in adult female mice for the arcuate nucleus of the hypothalamus (ARN), the dorsal raphe nucleus (DRN) of the midbrain, the liver (endoderm-derived), and skeletal muscle (mesoderm derived). Neuronal circuits in the ARN regulate the endocrine system, feeding, energy expenditure, and blood glucose homeostasis (Gao and Horvath, 2007; Sternson, 2013), while the DRN, a major serotonergic nucleus, influences stress and anxiety, arousal, feeding, reward, social behaviors, and pain (Challis et al., 2013; Dölen et al., 2013; Lowry et al., 2008; Michelsen et al., 2007; Monti, 2010; Wang and Nakai, 1994). By comparing imprinting in the brain to the liver and muscle, we examine the prevalence of canonical and noncanonical imprinting effects in different tissue types. By comparing the ARN and DRN, we determine whether imprinting differs between brain regions with important roles in human health. Our study reveals that

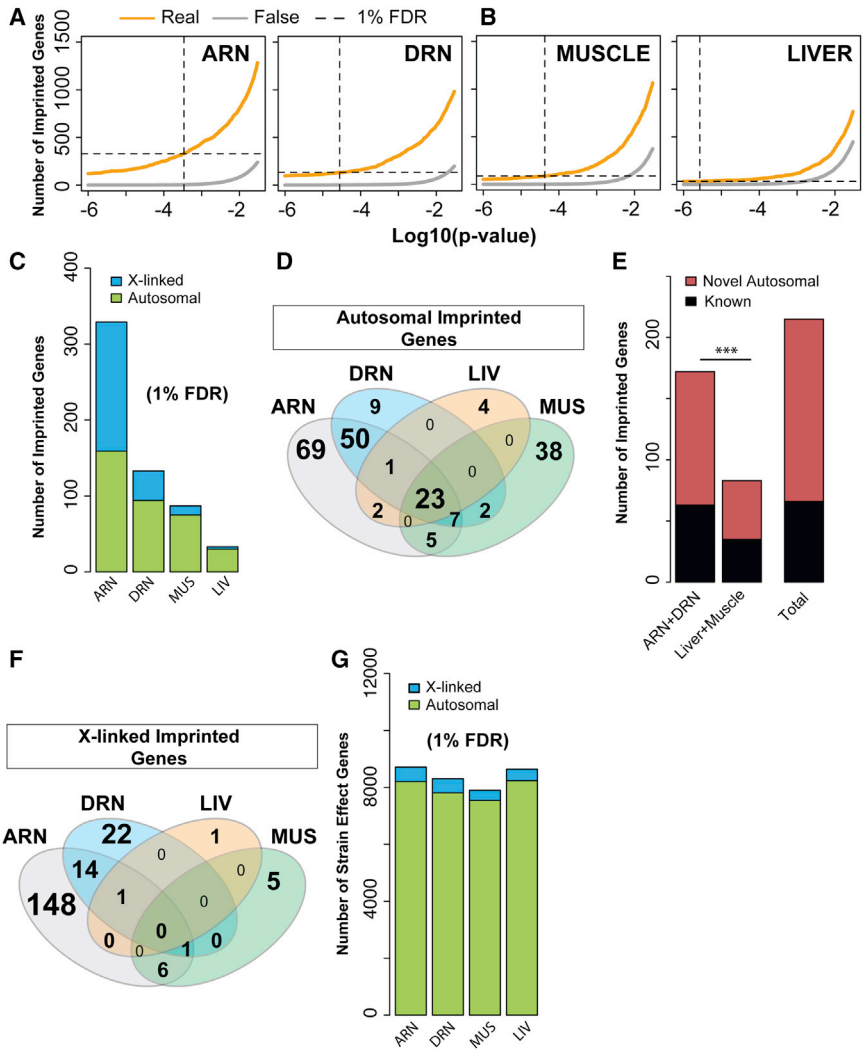

Figure 1. Detection of Imprinting Effects in the Adult Female ARN, DRN, Liver, and Muscle

(A and B) Number of imprinted genes detected by RNA-seq (orange line) and the estimated false-positives (gray line) at different p value cutoffs for the ARN, DRN, muscle, and liver (dashed line is 1% FDR).

(C) Number of autosomal (green bars) and X-linked (blue bars) imprinted genes in each tissue at the 1% FDR.

(D) Venn diagram of autosomal imprinted genes detected in each tissue at the 1% FDR.

(E) Number of novel (maroon bar) and known (black bar) autosomal imprinted genes uncovered in the ARN and DRN (neural) compared to the muscle and liver (non-neural), as well as the total number in all tissues.

(F) Venn diagram of X-lined imprinted genes detected at the 1% FDR cutoff in each tissue.

(G) Number of autosomal and X-linked genes that exhibit genetic strain effects in each tissue at the 1% FDR.

noncanonical imprinting effects are tissue specific and impact a few hundred autosomal and X-linked genes. We perform extensive independent validation studies that support our findings and demonstrate that noncanonical imprinting occurs in wild-derived outbred populations and involves allele-specific chromatin modifications. At the cellular level, noncanonical imprinted genes exhibit allele-specific expression effects in discrete subpopulations of neurons in the brain. These effects influence multiple genes in the monoamine pathway and cause parent-of-origin effects on offspring behavior for inherited heterozygous mutations in *tyrosine hydroxylase* (*Th*). Our results have important implications for understanding the genetic and epigenetic architecture underlying brain function and complex phenotypes.

RESULTS

Discovery of Novel and Tissue-Specific Imprinting Effects in Adult Female Mice

To detect imprinting effects in the ARN, DRN, liver, and muscle, we generated adult female F1 hybrid offspring from reciprocal crosses of CastEiJ (Cast) and C57BL/6J (B6) inbred strains and performed RNA-seq to profile the transcriptome of the initial (F1i: Cast mother × B6 father) and reciprocal (F1r: B6 mother × Cast father) hybrid offspring. We use base calls at SNP sites to distinguish expression from maternal and paternal alleles, as previously described (Gregg et al., 2010a, 2010b). For each tissue, we perform eight to nine biological replicates for each cross and deep sequencing, generating 80–100 million 59-bp single-end reads per replicate (Table S1). We made many advances to improve our methodology for detecting imprinting effects as detailed in the Supplemental Information (Figure S1). With these methods, we analyzed the ARN, DRN, liver, and muscle of adult female mice and determined the number of imprinted genes detected across a range of p value cutoffs ($p = 1 \times 10^{-6}$ to $p = 0.1$) (Figure 1A). The number of false-positives was estimated using a permutation test (Figure S1) and revealed that hundreds of genes exhibit significant imprinting effects in the ARN and DRN (Figure 1A), but fewer exist in the muscle and very few in the liver (Figure 1B). For each data set, we identified the p value cutoff that yields a conservative 1% false discovery rate (FDR) to define a high confidence set of imprinted genes (Figures 1A–1C). We identified 328 imprinted genes in the ARN, of which 158 are autosomal and 170 are X-linked (Figure 1C). We found that the ARN has 79% more autosomal imprinted genes than the DRN (93 imprinted genes), 110% more than the muscle (75 imprinted genes), and over 5-fold more than the liver (30 imprinted genes) (Figures 1C and 1D). Out of the 69 imprinted genes detected specifically in the ARN (Figure 1D), 48 genes (70%) showed the same direction of allele bias in the DRN,

but the magnitude of the bias was stronger in the ARN (ARN mean allele bias, 65%; DRN mean allele bias, 16%).

Our analysis uncovered autosomal imprinting effects that are specific to each tissue type (Figure 1D). We found over twice as many autosomal imprinted genes in the brain (ARN + DRN: 172 genes) compared to the nonneural tissues (muscle + liver: 83 genes), which is a significant difference ($p = 7.5 \times 10^{-5}$, Fisher's exact test) (Figure 1E). At the 1% FDR cutoff, we further detected 198 X-linked genes in total, and 75% of these were specifically identified in the ARN (170 X-linked genes) (Figures 1C and 1F). Thus, both autosomal and X-linked imprinting effects are enriched in the brain, and highly enriched in the ARN.

We compiled a list of 151 accepted imprinted genes from available public repositories (Schulz et al., 2008) and found that 98 are ensembl-annotated for the mouse. From this list, we determined that 142 of the 209 autosomal imprinted genes we identified are not among the previously annotated imprinted genes, while 66 are known. Interestingly, 79% of the unannotated imprinted genes were found in the brain only (Figure 1E). To determine whether these tissue differences are specific to imprinting, we analyzed allele expression effects in our hybrid data that arise due to genetic differences between Cast and B6 alleles (strain effects). We statistically detected strain effects with a generalized linear model (glm) that tests for a main effect of the strain of the allele, rather than the parental origin. This approach revealed that the majority of autosomal and X-linked genes exhibit a significant bias to express either the Cast or B6 allele in each tissue (Figure 1G, 1% FDR). Thus, the tissue differences for imprinting, which involve enrichments in the brain and a paucity of effects in the liver, do not occur for strain-related genetic allelic effects.

As detailed in the Supplemental Information, we can gain insights into the sensitivity of our methods by taking advantage of the known Xm expression bias in somatic tissues of female mice (Calaway et al., 2013; Chadwick and Willard, 2005; Fowlis et al., 1991; Gregg et al., 2010a; Wang et al., 2010). Between 80%–90% of X-linked genes exhibit a maternal allele expression bias in each of the four tissue types (Figures S2A and S2B). Thus, by evaluating the proportion of maternally biased X-linked genes that are detected at the 1% FDR, we can gain insights into the sensitivity of our methods (Figure S2). For the ARN, we found that 170 (35%) of the 492 total expressed and maternally biased X-linked genes are statistically detected as imprinted (Figure S2C). In the DRN, 38 (8%) of the 499 maternally biased X-linked genes are detected. For the liver and muscle, only three (0.7%) and 12 (2%) of the 421 and 414 maternally biased X-linked genes are detected, respectively. By relaxing the cutoff to a 20% FDR, we statistically detect the maternal bias for over 70% of maternally biased X-linked genes in the ARN and DRN. Thus, at the 1% FDR cutoff, our screen is not saturated and is powered to discover imprinting effects that are similar to the most robust maternally biased X-linked genes in the ARN. The results of our transcriptome-wide imprinting analysis are presented in Table S2.

Comparison of Canonical and Noncanonical Imprinting Effects

Next, we set out to compare the prevalence of autosomal canonical versus noncanonical imprinting effects. We define canonical imprinted genes as those that have at least 99% of expression or more arising from one parental allele in at least one tissue type, indicating allele silencing (Table S3). The Illumina sequencing error rate is estimated to be ~0.01%–0.1% (Loman et al., 2012; Meacham et al., 2011), and there is a one in four chance that an error will result in a B6 read being assigned as a Cast read (or visa versa) at a given SNP site. Thus, our 1% expression cutoff for allele-silencing effects is slightly higher than the expected background of ~0.025%. We classify all imprinted genes with greater than 1% of expression arising from the repressed allele as noncanonical, since they exhibit an allele expression bias. For example, *Peg3* is a canonical imprinted gene that expresses the paternal allele and silences the maternal allele in all tissues types (Figure 2A). In contrast, *Ago2* is a noncanonical imprinted gene that exhibits a *bias* to express the maternal allele in the ARN and DRN but not the liver or muscle (Figure 2B). We found a total of 24 canonical imprinted genes that exhibit allele silencing in at least one tissue (Figure 2C). In contrast, we found 186 autosomal genes that exhibit a significant bias to express either the maternal or paternal allele, and 142 of these have not previously been annotated (Figure 2D). Therefore, noncanonical imprinting effects are ~8-fold more prevalent than strict canonical imprinting effects.

Interestingly, 79% of canonical imprinted genes are expressed and imprinted in both neural and non-neural tissues (Figure 2C), but only 12% of noncanonical imprinted genes meet these criteria (Figure 2D). We further found that 64% of noncanonical imprinted genes are specific to the brain, 20% are specific to the muscle, and only 2% are specific to the liver (Figure 2D). Particularly striking is that 37% of noncanonical imprinted genes are specific to the ARN. Thus, unlike most canonical imprinting effects, noncanonical imprinting effects are highly tissue specific.

Canonical imprinted genes are typically located in gene clusters in the genome, which are defined by shared regulatory elements. We prospectively defined "clustered" and "remote" imprinted genes according to whether they are located within 1 Mb of another imprinted gene in the genome (Tables S3 and S4). As expected, we found that 92% (22 out of 24) of canonical imprinted genes are located in a cluster (Figure 2E). In contrast, only 57% of noncanonical imprinted genes are located in a cluster, while 43% reside in remote regions of the genome that are not close to other imprinted genes (Figure 2E). In total, we found evidence for 24 candidate imprinted gene clusters on 12 chromosomes (Table S4). Our results reveal that noncanonical imprinting arises both near canonical imprinted gene clusters and in novel genomic regions.

Noncanonical Imprinting Effects Can Arise Independently from Canonical Imprinting

Our results above indicate that noncanonical imprinted genes are not simply bystanders in close proximity to canonical imprinted genes, since many reside in novel regions of the genome. Here, we further investigated the relationship between canonical and noncanonical imprinted genes. For example, *Plagl1* is a canonical PEG (paternally expressed gene) in a micro-imprinted domain that is not thought to involve a gene cluster (Iglesias-Platas et al., 2013). A neighboring gene, called *Phactr2*, has been

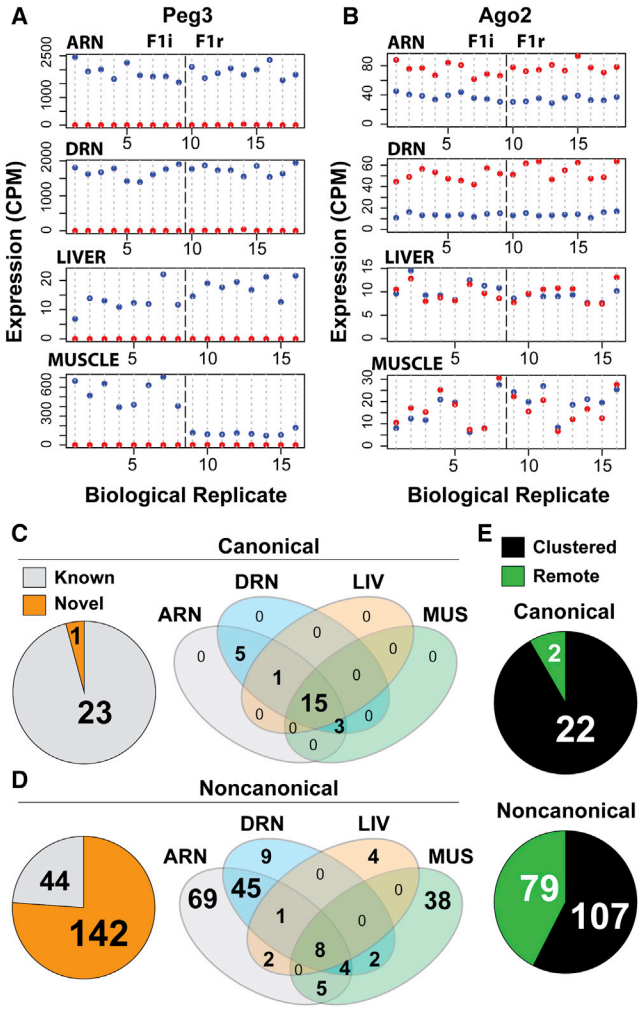

Figure 2. Comparison of Canonical and Noncanonical Imprinting Effects

(A and B) Examples of canonical (A, *Peg3*) and noncanonical (B, *Ago2*) imprinting in the ARN, DRN, liver, and muscle detected by RNA-seq. *Peg3* exhibits silencing of the maternal allele (red dots) and expression of the paternal allele (blue dots) in all tissues and biological replicates for F1i and F1r hybrid offspring (ARN, n = 9; DRN, n = 9; liver, n = 8; muscle, n = 8). *Ago2* exhibits a maternal bias in the ARN and DRN and no effect in the liver or muscle.

(C and D) Total number of known and novel canonical (C) and noncanonical (D) imprinted genes discovered and a Venn analysis of the tissues in which the genes were found.

(E) Number of canonical and noncanonical imprinted genes in clusters (clustered) compared to novel genomic regions (remote).

previously shown to exhibit noncanonical imprinting in the mouse placenta (Wang et al., 2011). In our analysis, we uncovered a maternal bias for four genes near *Plagl1*, which include *Sf3b5*, *Ltv1*, *Phactr2*, and *Fuca2* (Figure S3A). Interestingly, *Plagl1* exhibits canonical imprinting in all four tissues (Figure S3B); however, the neighboring noncanonical imprinting effects are highly tissue specific. *Sf3b5* and *Ltv1* exhibit a maternal allele bias specifically in the ARN (Figures S3C and S3D). *Phactr2* exhibits a maternal bias in the ARN and DRN, but not the liver or muscle (Figure S3E). Finally, *Fuca2* exhibits a maternal bias in the ARN and muscle, but not the DRN or liver (Figure S3F). The strength of the maternal bias for these effects does not simply decrease as a function of the distance from *Plagl1*, since *Phactr2* exhibits a stronger bias than either *Sf3b5* or *Ltv1*. Pyrosequencing confirmed that *Fuca2* exhibits a significant maternal bias in the ARN, but not the liver, in Cast × B6 and PWD/J × A/J hybrid offspring (Figure S3G). We refer readers to a second representative example at the *Inpp5f* locus (Figures S3H–S3N and Supplemental Results). A complete annotation of noncanonical imprinting effects near canonical imprinted genes is presented in Table S4. Out of the 18 gene clusters that contained canonical and noncanonical imprinted genes, 15 clusters contain maternally biased noncanonical imprinted genes only and three contain paternally biased genes only (Table S4). The *Peg3-Usp29* gene cluster has both maternally and paternally biased noncanonical imprinting effects depending on the tissue, and we validated these effects for *Clcn4*, which is maternally biased in brain and paternal in liver (Table S5).

We further identified 79 noncanonical imprinted genes in regions of the genome that do not contain other imprinted genes (Figure 2E). For example, *Nhlrc1* is located on chromosome 13 near a differentially methylated region (Xie et al., 2012). We found that *Nhlrc1* exhibits noncanonical imprinting involving a paternal bias in the ARN and DRN, but not the liver or muscle (Figures S4A and S4B). The genes surrounding *Nhlrc1* do not exhibit imprinting in any tissue (Figure S4A). Similarly, *Acrbp* exhibits a paternal bias in the ARN and DRN, but not the liver or muscle (Figures S4C and S4D). We also found similar effects in the muscle. For example, *Gbp7* (Figures S4E and S4F, chromosome 3) and *643054M08Rik* (Figures S4G and S4H, chromosome 8) exhibit a paternal and maternal bias, respectively, in muscle only. The neighboring genes do not exhibit imprinting in any of the tissues (Figures S4E and S4G). We confirmed tissue-specific imprinting for these examples and others by pyrosequencing in Cast × B6 and/or PWD/J × A/J hybrid mice (Table S5). Therefore, noncanonical imprinting effects arise independently from canonical imprinting in a highly tissue-specific manner.

Noncanonical Imprinting Effects Are Reproducible in Multiple Genetic Backgrounds

We performed pyrosequencing validations for 64 imprinted genes identified in our RNA-seq study, including 62 noncanonical imprinted genes selected from a wide range of p value cutoffs in the data. We assayed these genes in one or more tissue types, carrying out a total of 136 validation experiments involving four to eight biological replicates each. We successfully validated imprinting for 89% (57/64) of the genes tested in at least one tissue type. Out of the 136 validation experiments performed, 106 were carried out for 57 genes using Cast × B6 hybrid mice (Figure 3A; Table S5). To ascertain whether noncanonical imprinting effects are conserved across genetic backgrounds, we performed 30 further validation experiments for 23 genes with PWD/J × A/J hybrid mice (Figure 3A; Table S5).

In our validation studies using Cast × B6 hybrid mice, 17 out of 106 pyrosequencing results disagree with the RNA-seq results.

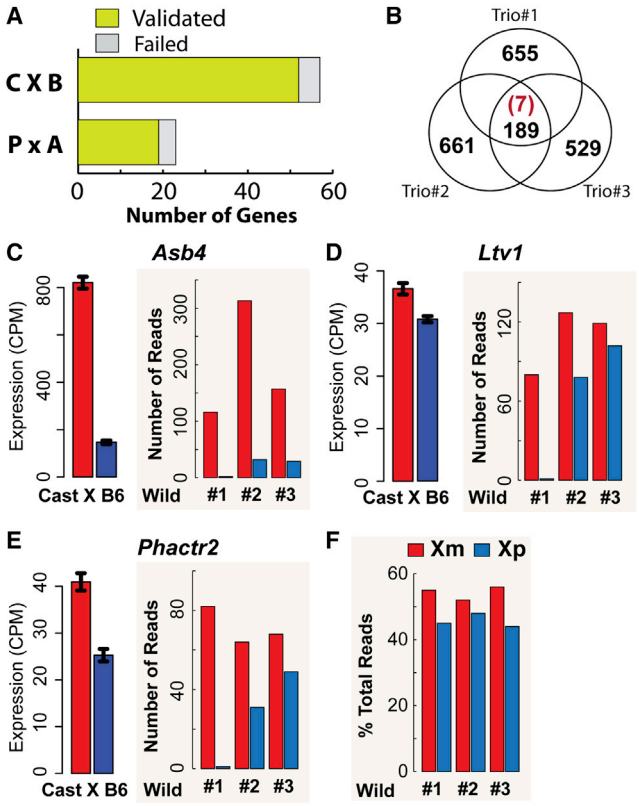

Figure 3. Noncanonical Imprinting Effects Are Highly Reproducible and Conserved in Outbred, Wild-Derived Mice

(A) Summary of pyrosequencing validation experiments in Cast × B6 (C × B) and PWD/J × A/J (P × A) hybrid offspring reveals high validation rates.

(B) Venn diagram of the number of expressed genes with SNPs for each wild-derived daughter. Out of the 189 SNP-containing genes shared between the trios, seven are imprinted genes identified in the ARN in hybrid mice.

(C–E) *Asb4*, *Ltv1*, and *Phactr2* are noncanonical MEGs with biased expression of the maternal allele (red) in Cast × B6 hybrid mice as revealed by RNA-seq. A similar maternal bias is present in each of the wild-derived daughters (1, 2, and 3).

(F) The percentage of total reads derived from Xm versus Xp alleles in the wild-derived daughters reveals an Xm expression bias.

Eight of these cases involve false-negatives in which the imprinting effect is not statistically significant by RNA-seq but is significant by pyrosequencing. Only nine cases involve potential false-positives in which imprinting is detected by RNA-seq but is not statistically significant by pyrosequencing. Finally, out of the 30 validation experiments performed in PWD/J × A/J mice, 87% (26/30 genes) agree with the RNA-seq data from Cast × B6 hybrid mice. In total, we confirmed the imprinting status for 46/50 genes tested in the ARN, 14/14 genes in the DRN, 21/25 genes in muscle, and 20/21 genes in the liver. We validated tissue-specific imprinting for 15 noncanonical imprinted genes that exhibit imprinting in the ARN, but not the liver, as well as seven genes that exhibit imprinting in the muscle only. Thus, our RNA-seq results are highly reproducible across different genetic backgrounds, and we confirmed the tissue-specific nature of noncanonical imprinting.

It is unknown whether noncanonical imprinting effects exist in wild-derived, outbred populations. To address this issue, we obtained Idaho wild-derived mice that have been maintained in captivity as an outbred colony (Miller et al., 2002). We generated three separate parent-offspring trios and harvested RNA from the hypothalamus of each parent and one daughter for each trio for analysis by RNA-seq (see the Supplemental Information). We found 189 genes that had distinguishing SNPs in all three trios and could therefore be assessed for reproducible allele-specific expression effects (Figure 3B). Out of these 189 genes, seven were identified as noncanonical imprinted genes in the ARN of F1 hybrid mice: *Asb4*, *Trappc9*, *Herc3*, *Ltv1*, *Phactr2*, *Cobl*, and *Igf2r*. In the wild-derived daughters, we found a similar noncanonical maternal bias for all of these genes except *Igf2r*, which did not exhibit imprinting (Table S6). For example, in daughter 1, *Asb4*, *Ltv1*, and *Phactr2* are almost exclusively expressed from the maternal allele, and a maternal bias is present in daughters 2 and 3 (Figures 3E and 3F). Finally, in the hybrid mice we also observed a bias to express alleles on the Xm (Figure S2), and to evaluate this phenomenon in the wild-derived mice we determined the percentage of overall expression that arises from the Xm versus the Xp in each daughter (Table S6). In all three wild-derived daughters, we found an Xm bias (Figure 5H), and the bias persists if we relax the quality score cutoff for the SNP calls to increase the total number of SNP sites examined or increase the stringency by only analyzing sites that are homozygous between the parents (data not shown). Overall, our results reveal that noncanonical imprinting effects are present in natural, outbred populations.

Tissue and Gene-Specific Imprinting Effects Arise on the X Chromosome

In females, imprinting effects can arise on the X chromosome. As noted above, at a 1% FDR, we detected imprinting effects for 198 X-linked genes, and 86% of these genes (170 genes) were detected in the ARN, compared to only 20% in the DRN, 6% in the muscle, and 1.5% in the liver (Figures 1C and 1F). Scatterplots of the mean allele bias versus the p value for imprinting for X-linked genes reveal that most X-linked genes exhibit a mean maternal bias in each of the tissues; however, the robustness of the bias appears highly gene and tissue specific (Figure 4A). Gene level imprinting effects are known to occur on the X chromosome; for example, *Xlr3b*, *Xlr4b*, and *Xlr4c* are only expressed from the Xm in some tissues (Davies et al., 2005; Raefski and O'Neill, 2005). In our study, we found that *Xlr3a*, *Xlr3c*, and *Xlr3e* exhibit the strongest maternal effects in all tissues (Figure 4A), though the statistical scores are low due to the low expression level of these genes. We further found preferential expression of the paternal *Xist* allele in all four tissues (Figure 4A), which is consistent with a bias to silence the Xp and express the Xm.

Our scatterplots also indicate X-linked genes that exhibit maternal allele expression biases in each tissue, as well as genes that do not (Figure 4A). For example, *Hmgb3* exhibits a very modest maternal bias in the ARN and DRN, and no effect in the liver and muscle (Figure 4A). In contrast, *Il13ra1* exhibits a relatively robust maternal bias in the ARN and DRN compared

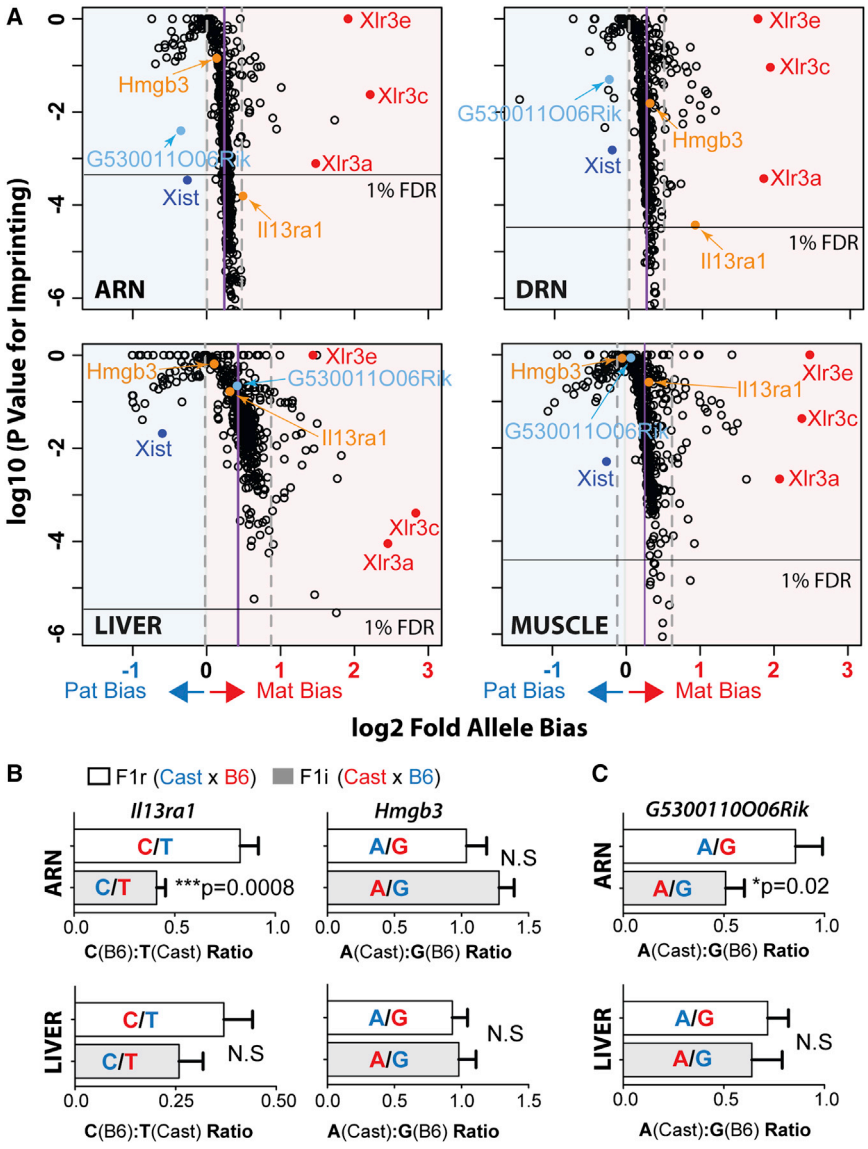

Figure 4. Tissue-Specific Imprinting Effects on the X Chromosome

(A) Scatterplots of paternal (blue side) and maternal (red side) allele expression biases (log2-fold bias) versus the p value (log10) for imprinting effects for all X-linked genes. Most X-linked genes exhibit a maternal allele expression bias (mean allele bias is indicated by the purple line; gray dashed lines indicate 1 SD from this mean). The maternally biased *Xlr* genes are indicated in red, and *Xist* is indicated in dark blue. Examples of tissue-specific X-linked imprinting effects are indicated for the MEGs, *Hmgb3* and *Il13ra1* (orange), and the PEG, *G530011O06Rik* (light blue). (B and C) Pyrosequencing validations in Cast × B6 F1 hybrid offspring. (B) *Il13ra1* and *Hmgb3* demonstrate a significant maternal bias for *Il13ra1* in the ARN, but not the liver, and *Hmgb3* does not exhibit a significant maternal bias in either tissue. (C) *G530011O06Rik* exhibits a paternal bias in the ARN, but not the liver (n = 8, mean ± SEM, one-tailed t test).

to *Hmgb3* (Figure 4A). Additionally, *G530011O06Rik* exhibits a paternal bias in the ARN and DRN, but not in the liver or muscle. Pyrosequencing confirmed the gene and tissue-specific noncanonical imprinting effects for these genes (Figures 4B and 4C). Pyrosequencing in Cast × B6 hybrid mice further validated brain-specific imprinting effects for the X-linked genes *Maoa*, *Bcor*, *C77370*, and *Gspt2* (Table S5). We also validated *Bcor* and *Maoa* in PWD × A/J hybrid offspring, revealing that these effects are present in different genetic backgrounds (Table S5).

Twelve genes are known to escape X-inactivation in the mouse (Yang et al., 2010), and we found that these genes also appear to exhibit tissue-specific imprinting effects (Figure S5A). For example, *Kdm6a* exhibits a modest maternal bias in the ARN, but no effect in the DRN, liver, or muscle. Pyrosequencing confirmed the maternal bias in the ARN and the absence of this bias in the DRN in Cast × B6 hybrids (Figure S5B). In PWD × A/J hybrids, we found a significant maternal bias for *Kdm6a* in both brain regions (Figure S5C). Thus, genes that are known to escape X-inactivation can exhibit a maternal allele bias, though it is unclear whether the observed effects are related to gene-specific imprinting or changes to X-inactivation escape.

Our findings detail maternal allele biases for many X-linked genes in females (Figure S2). We also tallied the total number of maternally versus paternally biased autosomal genes in each tissue (Figure S5D). Interestingly, we uncovered 107 more PEGs than MEGs on chromosome 1 in the DRN, which is a statistically significant overall paternal bias (Figure S5D, p = 0.002, Fisher's exact test). These results suggest biased maternal and paternal influences over X-linked and autosomal gene expression, respectively.

Noncanonical Imprinting Is Associated with Allele-Specific Histone Modifications

To ascertain whether noncanonical imprinting effects detected at the transcriptome level are associated with allele-specific chromatin modifications, we isolated chromatin from the hypothalamus of F1i and F1r Cast × B6 hybrid offspring and performed chromatin immunoprecipitation (ChIP). We targeted the transcriptionally permissive and repressive histone modifications H3K9ac and H3K9me3, respectively (Dindot et al., 2009; Singh et al., 2010), and focused on promoter regions by identifying SNPs within ±300 bp from the transcriptional start site for four canonical imprinted genes, six noncanonical imprinted genes, and one non-imprinted control gene (Table S7).

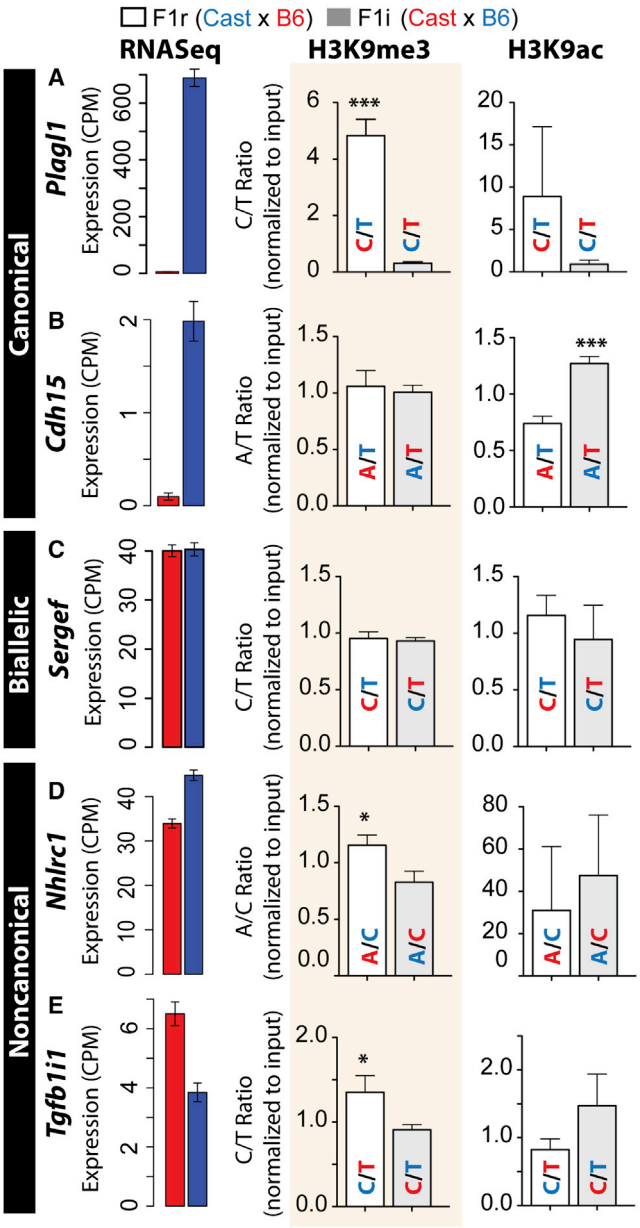

Figure 5. Chromatin Immunoprecipitation and Pyrosequencing Reveals Allele-Specific Repressive Chromatin at Noncanonical Imprinted Loci

(A and B) RNA-seq indicates that *Plagl1* (A) and *Cdh15* (B) are canonical PEGs in the ARN. ChIP-pryo analysis in Cast × B6 hybrid mice targeting SNPs sites in the promoter region for *Plagl1* reveals a significant enrichment for H3K9me3 on the repressed maternal allele and no significant enrichment for H3K9ac on either allele. In contrast, *Cdh15* exhibits a significant enrichment for H3K9ac on the expressed paternal allele and no significant enrichment for H3K9me3 on the repressed maternal allele. Enrichments are normalized to input controls.

(C) *Sergef* is a negative control gene that does not exhibit imprinting and does not exhibit maternal or paternal allele-specific enrichments for H3K9me3 or H3K9ac.

(D) *Nhlrc1* is a remote noncanonical PEG and ChIP-pyro reveals enriched H3K9me3 on the partially repressed maternal allele and no enrichment for H3K9ac on either allele.

(E) *Tgfb1i1* is a clustered noncanonical MEG and ChIP-pyro reveals a significant enrichment for H3K9me3 on the repressed paternal allele and no significant enrichment for H3K9ac on either allele. n = 6–8, two-tailed t test, mean ± SEM, ***p < 0.001, *p < 0.05.

For the canonical imprinted genes, *Plagl1* (Figure 5A), *Magel2,* and *Meg3* (Table S7), pyrosequencing revealed a significant enrichment for H3K9me3 on the silenced allele, but no enrichment for H3K9ac on the expressed allele (Figure 5A; Table S7). In contrast, for *Cdh15*, we found a significant enrichment for H3K9ac on the expressed allele but did not detect H3K9me3 enrichment on the silent allele (Figure 5B). As a negative control, we analyzed *Sergef*, which expresses the maternal and paternal alleles equally, and no allelic differences in H3K9me3 or H3K9ac enrichment were observed for this gene (Figure 5C).

Next, we analyzed six noncanonical imprinted genes, including *Nhlrc1* (PEG), *Tgfb1i1* (MEG, maternally expressed gene), *Slc25a29* (PEG), *Eif2c2* (MEG), *Trappc9* (MEG), and *Bcl2l1* (PEG). We found a significant enrichment for H3K9me3 on the repressed allele for five out of six genes (Table S7). For example, *Nhlrc1* and *Tgfb1i1* exhibit preferential expression of the paternal and maternal alleles, respectively (Figures 5D and 5E). We found a significant enrichment for H3K9me3 on the maternal allele for *Nhlrc1* (Figure 5D) and on the paternal allele for *Tgfb1i1* (Figure 5E), consistent with the repression of these alleles. Similar effects were detected for *Ago2* and *Bcl2l1*, but not for *Slc25a29* (Table S7). For *Trappc9*, we found significant H3K9ac enrichment on the maternal allele and H3K9me3 on the paternal allele (Table S7). Therefore, like canonical imprinting, noncanonical imprinting effects are associated with allele-specific chromatin modifications.

Noncanonical Imprinted Genes Exhibit Allele-Specific Expression in Subpopulations of Neurons

We tested several models to gain insights into the mechanisms underlying noncanonical imprinting effects at the cellular level. First, maternal or paternal allele-specific expression biases could be due to distinct, but overlapping transcripts from maternal versus paternal alleles (Figure 6A). However, as detailed in the Supplemental Results (and Figures S6A–S6D), we devised an approach to analyze imprinting at the transcript level and determined that *H13*, *Commd1*, *Trappc9*, *Herc3*, *Inpp5f*, *Blcap*, *Mest*, *Ube3a*, and *Gnas* are the only genes with overlapping, allele-specific isoforms (BH adjusted p value <0.01). Therefore, most noncanonical imprinting effects are not due to this phenomenon.

Alternatively, noncanonical imprinting effects could be due to (1) an allele expression bias in each cell (Figure 6B), (2) skewed random monoallelic expression effects (Figure 6C), or (3) allele silencing in a subpopulation of cells (Figure 6D). To test these possibilities, we devised an approach to resolve allele-specific expression at the cellular level using RNAscope in situ hybridization probes. Probes were designed against intronic regions to detect nascent RNA arising from each allele in the nucleus of cells in tissue cryosections of the ARN and DRN. We first evaluated this approach for the canonical MEG, *Meg3*. Our analysis is performed in isogenic female B6 mice, and we observe a single focal site of allele transcription in over 80% of positive cells,

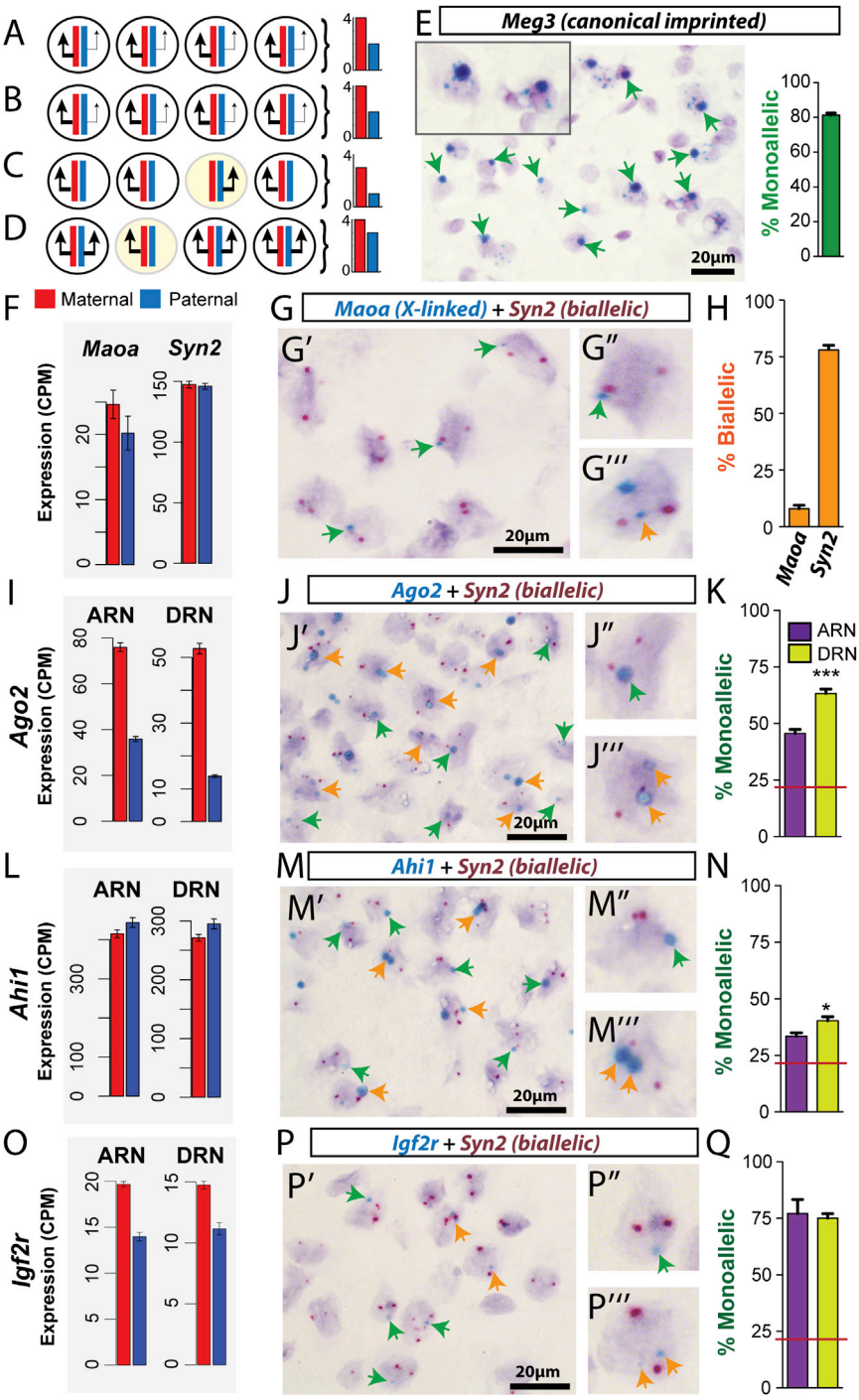

Figure 6. RNAscope Detection of Nascent RNA Reveals Subpopulations of Monoallelic Cells for Noncanonical Imprinted Genes In Vivo

(A–D) Models of noncanonical imprinting effects at the cellular level (see main text).

(E) Intronic probe targeting nascent RNA for *Meg3* (canonical imprinted) reveals monoallelic expression in cells of the DRN (green arrows). Hematoxylin nuclear counterstaining reveals nuclei in cryosections. The proportion of monoallelic cells is indicated in the bar graph (n = 3).

(F–H) RNA-seq reveals maternal bias for the X-linked gene, *Maoa*, and equal expression of the maternal and paternal alleles for *Syn2* (autosomal, ARN data shown) (F). Nascent RNA in situ (blue) in the ARN reveals largely monoallelic (P′ and P″, green arrows) and very few biallelic (P‴, orange arrows) *Maoa*$^+$ cells. In contrast, *Syn2* (dark red) expresses both alleles in most positive cells. Bar plot indicates the percentage of *Maoa*$^+$ and *Syn2*$^+$ cells that are biallelic (Q, n = 3).

(I–Q) RNA-seq data indicate maternal and paternal allele expression for *Ago2* (I), *Ahi1* (L), and *Igf2r* (O). Intronic probes reveal subpopulations of biallelic (orange arrows) and monoallelic (green arrows) cells in the ARN for *Ago2* (J), *Ahi1* (M), and *Igf2r* (P) indicated by blue staining. *Syn2* staining (biallelic control) is dark red. Bar plots indicate the percentage of monoallelic cells out of the total positive cells in the ARN and DRN (K, N, Q; n = 3–6, two-tailed t test, red line indicates *Syn2* estimated false monoallelic background). Mean ± SEM, *p < 0.05, ***p < 0.001.

consistent with canonical imprinting for this gene (Figure 6E). We further noted small speckles outside of the primary nuclear site of allele expression and demonstrate that this staining is due to some intron retention in the nascent RNA (Figures S7A–S7E). To resolve this issue, we developed methods in which probes are designed to specifically target rapidly processed introns (Figures S7A–S7E). With our approach, we can resolve allelic expression at the cellular level for any gene.

We analyzed allelic expression effects for a nonimprinted, biallelic control gene, *synapsin II* (*Syn2*), which is ubiquitously expressed in neurons and found that *Syn2* exhibits biallelic expression in ~77% of neurons (n = 3, see *Syn2* staining in Figures 6F–6H). In contrast, the X-linked gene *Maoa* exhibits biallelic expression in fewer than 8% of *Maoa*$^+$ neurons, as expected due to the effects of random X-inactivation (Figures 6F–6H). We suspected that the apparent monoallelic *Syn2*$^+$ cells are artifacts from partial nuclei cut during cryosectioning. Indeed, confocal Z-stacks of 14-μm sections revealed that 30%–35% of DAPI$^+$ nuclei are partial (Figures S7F and S7G). Therefore, based on the *Syn2* biallelic control, we conclude that our method has a background effect in which ~23% of monoallelic cells are potentially false due to sectioning artifacts.

Next, we used our approach to analyze allelic expression effects for noncanonical imprinted genes and performed double labeling with *Syn2*, as an internal biallelic control and neuron marker. We first analyzed *Ago2*, which exhibits a 2-fold maternal

allele bias in the ARN and 3-fold maternal bias in the DRN (Figure 6I). We found that 46% and 63% of *Ago2*$^+$ cells are monoallelic in the ARN and DRN, respectively, revealing significantly more monoallelic cells in the DRN, which has stronger imprinting (Figures 6J and 6K). *Ahi1* exhibits a paternal allele bias by RNA-seq, and we found that 34% and 40% of *Ahi1*$^+$ cells are monoallelic in the ARN and DRN, respectively (Figures 6L–6N). Finally, we found that *Igf2r* is a noncanonical MEG in the brain and determined that it exhibits monoallelic expression in ~75% of positive cells in the ARN and DRN (Figures 6O–6Q). Importantly, the number of monoallelic cells detected for *Ago2*, *Ahi1*, and *Igf2r* is at approximately 2-fold higher, or more, than the background of our approach (red line in Figures 6H, 6K, and 6N), and we clearly identify monoallelic effects in neurons that are biallelic for *Syn2* (Figures 6G″, 6J″, and 6M″), indicating bona fide allele-specific expression effects. To further confirm our findings, we devised a fluorescent staining and confocal imaging strategy to detect whole nuclei and determined that bona fide monoallelic and biallelic cellular subpopulations exist for cells with fully intact nuclei for both *Ahi1* (Figure S7H) and *Ago2* (Figure S7I). Based on these findings, we conclude that autosomal noncanonical imprinted genes exhibit allele-specific expression effects in subpopulations of neurons in the brain.

Noncanonical Imprinting Effects Influence the Monoamine Pathway and Offspring Phenotypes

Gene ontology analysis and literature searches provided us with insights into the biological pathways that contain imprinted genes. In the ARN and DRN, we discovered several noncanonical imprinted genes with roles in monoamine signaling, including tyrosine hydroxylase (*Th*, MEG), *Ddc* (MEG), *Maoa* (X-linked MEG), *Tgf1b1i* (MEG), and *Ahi1* (PEG), as well as known canonical imprinted genes that influence monoamine signaling, including *RasGrf1* and the snoRNA, *HBII-52* (Figures 7A and 7B) (Doe et al., 2009; Fernández-Medarde and Santos, 2011). We used pyrosequencing to evaluate the imprinting status of the noncanonical imprinted genes in major monoaminergic nuclei, as well as *Dbh* (*dopamine beta-hydroxylase*), which regulates norepinephrine (NE) synthesis, and *Tph2* (*tryptophan hydroxylase*), which regulates serotonin synthesis. We performed our analysis in the ARN, DRN, ventral tegmental area (VTA), and the locus coeruleus (LC).

Our study revealed that *Dbh* and *Tph2* are not imprinted in the LC and DRN, respectively (Figure 7C). However, *Th* exhibits a significant maternal allele bias (Figure 7D, $p < 0.05$, main effect of cross, two-way ANOVA). The bias appears in the ARN, DRN, and LC, but not in the VTA, though this brain region difference did not result in a significant interaction effect between cross and brain region (Figure 7D). On the other hand, *Ddc* exhibits a maternal bias that is significantly different between brain regions (Figure 7E, $p < 0.0001$, interaction between cross and brain region). *Ddc* imprinting is strongest in the ARN and the LC, weaker in the DRN and is not significant in the VTA (Figure 7E, Tukey HSD post hoc test). *Tgfb1i1* interacts with the dopamine transporter (DAT) (Carneiro et al., 2002) and exhibits a significant maternal bias in each of the brain regions (Figure 7F). *Ahi1* can influence serotonin signaling (Wang et al., 2012) and exhibits a significant paternal bias in each brain region (Figure 7G). Next, we used RNAscope probes to analyze allelic expression at the cellular level for *Ddc* in B6 female mice. We found that the number of *Ddc*$^+$ monoallelic cells in the ARN is significantly greater than in the VTA (Figures 7H–7J). Therefore, more monoallelic cells are detected in the brain region with stronger imprinting.

Finally, we found subpopulations of *Th*$^+$ neurons in the brain that exhibit allele-specific expression effects (Figure 7K) and sought to test whether *Th* imprinting effects influence the impact of inherited mutations on offspring behavior. We obtained *Th* mutant mice on a B6 background and generated reciprocal *Th*$^{-/+}$ (maternal deletion) and *Th*$^{+/-}$ (paternal deletion) heterozygous offspring, as well as wild-type littermates. *Th* heterozygous mice are known to exhibit reduced catecholamine levels in the brain and significant behavioral changes (Kobayashi et al., 2000), and catecholamines influence motivated behaviors. We performed open-field testing to compare *Th*$^{-/+}$ and *Th*$^{+/-}$ offspring and observed a significant effect of the parental origin of the mutation in males and females, such that offspring with a mutated maternal allele spent more time in the center of the arena compared to offspring with a mutated paternal allele (Figure 7L). No difference was observed between the wild-type littermates (Figure 7M), and the total distance traveled was not different for any genotype (data not shown). In the sucrose intake test, a hedonic measure, we found that offspring with a mutated maternal allele (*Th*$^{-/+}$) consume significantly more sucrose solution compared to those with a mutated paternal allele (*Th*$^{+/-}$) (Figure 7N). No difference was observed between the wild-type littermates (Figure 7O). In summary, noncanonical imprinting influences genes in the monoamine pathway, in some cases the effects are brain region specific, and effects at a single locus can significantly, albeit modestly, influence the effect of inherited mutations on behavior.

DISCUSSION

Studies of imprinting have uncovered important insights into the genetic architecture of complex phenotypes, human disease, and the nature of epigenetic regulatory mechanisms (Adalsteinsson and Ferguson-Smith, 2014; Lawson et al., 2013; Peters, 2014). However, little is known about noncanonical imprinting effects that manifest as allele expression biases at the tissue level. Here, we devised a sensitive RNA-seq-based approach that accurately detects both canonical and noncanonical imprinting effects in two brain regions, skeletal muscle, and liver. Our study documents 210 autosomal imprinted genes in the adult female mouse, of which 142 are noncanonical imprinted genes. In addition, we uncovered tissue-specific imprinting effects that influence X-linked genes. Our findings demonstrate that noncanonical imprinting effects are highly enriched in the brain, are expressed independently from canonical imprinting effects, are reproducible across different genetic backgrounds of inbred mice, are conserved in wild-derived mice and involve allele-specific chromatin modifications. On the basis of these results, we conclude that noncanonical imprinting is a bona fide form of epigenetic allele regulation.

We provide evidence that autosomal noncanonical imprinted genes exhibit allele-specific expression effects in discrete subpopulations of neurons in the brain. The allele-specific

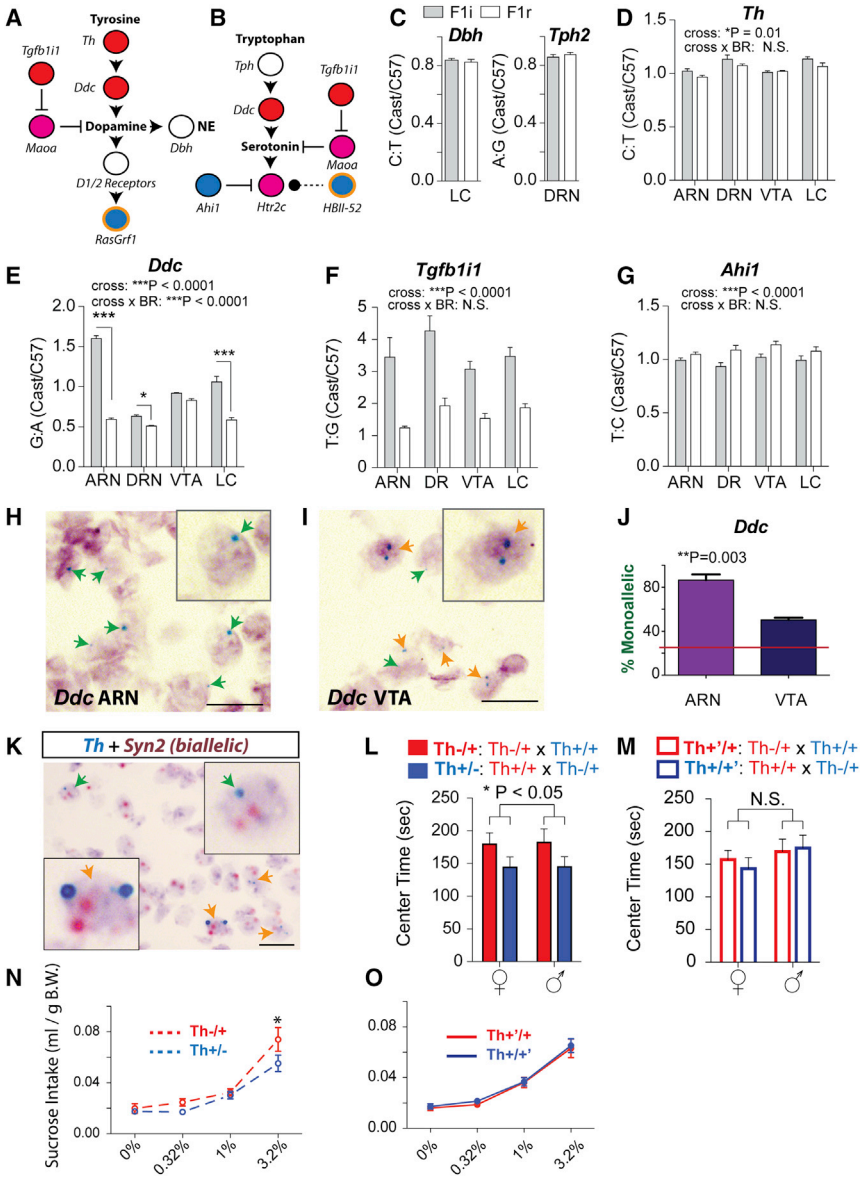

Figure 7. Noncanonical Imprinting in the Monoamine Pathway Causes Parent-of-Origin Effects for Inherited Mutations

(A and B) Summary of canonical (yellow border) and noncanonical (black border) MEGs (red) and PEGs (blue) in the catecholamine (A) and serotonin (B) pathways. X-linked MEGs indicated in pink.

(C) Pyrosequencing reveals that *Dbh* and *Tph2* are not imprinted in the LC and DRN, respectively (n = 8).

(D–G) Pyrosequencing for *Th*, *Ddc*, *Tgfb1i1*, and *Ahi1* in the ARN, DRN, VTA, and LC. All genes exhibit a significant main effect of cross revealing a noncanonical imprinting effect (n = 6–8, mean ± SEM, two-way ANOVA). Only *Ddc* exhibits a significant interaction between cross and brain region (BR), revealing brain region differences in the imprinting effect (n = 8). A Tukey HSD post-test determined that *Ddc* exhibits a significant maternal bias in the ARN, DRN, and LC, but not the VTA (*p < 0.05, **p < 0.01, **p < 0.001).

(H–J) *Ddc* nascent RNA in situ reveals monoallelic and biallelic subpopulations of neurons in the ARN (H) and VTA (I). A significantly larger proportion of Ddc^{+} cells exhibit monoallelic expression in the ARN compared to the VTA (J, n = 3, mean ± SEM, two-tailed t test, red line indicates *Syn2* estimated false monoallelic background). Scale bar, 20 μm.

(K) *Th* nascent RNA in situ (blue) reveals monoallelic and biallelic cells in the brain (ARN shown). Biallelic *Syn2* control in dark red.

(L and M) Total time in the center region for $Th^{+/-}$ and $^{-/+}$ females and males in the open-field task reveals a main effect of the parental origin of the mutant allele (n = 6–8, mean ± SEM, two-way ANOVA). (M) No difference is observed between the wild-type littermates (n = 8).

(N and O) Sucrose solution intake per gram of body weight (BW) at increasing sucrose concentrations reveals a significant increase in sucrose consumption for $Th^{-/+}$ compared to $Th^{+/-}$ offspring for the 3.2% sucrose solution (n = 13, *p < 0.05, mean ± SEM, Tukey HSD post test; data for males and females are pooled since no significant sex difference was detected). (O) No difference was detected between the wild-type littermates.

expression effects could involve highly cell-type-specific canonical imprinting, or alternatively, maternally or paternally skewed random monoallelic effects (Zwemer et al., 2012) or allelic bursting (Bahar Halpern et al., 2015). The relative proportion of monoallelic cells detected in B6 mice with our approach follows the relative strength of the imprinting effect at the tissue level for *Ago2*, *Ahi1*, and *Ddc* in hybrid mice. However, for *Igf2r*, we observed more monoallelic cells than might be expected based on the strength of the imprinting effect. One explanation is that biallelic and monoallelic cells express at different levels, and therefore the tissue-level allele bias is not directly proportional to the number of monoallelic cells. Additionally, some degree of skewed random allelic expression or allelic transcriptional bursting could influence the relationship between the tissue level allele expression bias and the number of monoallelic cells. Differences between hybrid and B6 mice could also contribute.

A deeper understanding of how noncanonical imprinting impacts defined sets of neurons in the brain will be essential to determine the specific brain functions and behaviors that are influenced. We report an initial analysis of the impact of *Th* noncanonical imprinting effects on behavior in the open-field and sucrose intake tasks and identified statistically significant, but modest effects. Further insights into the identity of the neurons that exhibit allele-specific *Th* expression effects are expected to reveal the brain functions that are most strongly impacted by *Th* imprinting. Interestingly, *Th* and *Ddc* exhibit similar patterns of imprinting across the major monoaminergic nuclei of the brain, with a relatively stronger maternal allele bias in the ARN and LC, weak effects in the DRN, and no effect in the

VTA. Given that these two enzymes regulate catecholamine synthesis, we expect that their combined imprinting effects additively influence specific aspects of brain function and behavior, which is an important area for future work. Gene ontology analysis of our data also indicates other possible synergistic relationships between different canonical and noncanonical imprinted genes in the regulation of neuron differentiation, metabolic processes, and cell signaling. Interestingly, we found that over 80% of all imprinted genes are noncanonical, and therefore noncanonical imprinting is the most prevalent form of imprinting in mice. Canonical imprinting is thought to be associated with a cost due to the fact that only a single allele is expressed and therefore heterozygosity cannot buffer against deleterious mutations (Otto and Goldstein, 1992). We speculate that the evolution of highly tissue- and cell-specific noncanonical imprinting effects that function by influencing multiple genes in a pathway reduces these costs to the offspring.

Our results reveal that most canonical imprinted genes exhibit imprinting in multiple tissue types, in agreement with a recent survey (Prickett and Oakey, 2012). We provide evidence that strict canonical imprinting involving allele silencing at the tissue level, occurs for 24 genes plus nine imprinted genes that have overlapping maternal and paternal transcripts. In contrast, noncanonical imprinting effects are highly enriched in the ARN, but rare in the liver. The enrichment for noncanonical imprinting in the ARN involves both autosomal and X-linked imprinting effects. The ARN plays central roles in the regulation of hunger, metabolism, glucose homeostasis, and the neuroendocrine system (Gao and Horvath, 2007; Sternson, 2013). Several studies have defined roles for canonical imprinted genes in the hypothalamus and in the regulation of feeding, metabolism, glucose homeostasis, and the neuroendocrine axis (Ivanova and Kelsey, 2011). Thus, canonical and noncanonical imprinting effects may have evolved under similar selective pressures.

Some studies have reported loss-of-imprinting in hybrid animals (Wolf et al., 2014), raising the concern that noncanonical imprinting is due to disrupted canonical imprinting mechanisms in hybrid mice. However, there are few examples of altered imprinting in Cast × B6 hybrid mice (Korostowski et al., 2012). In our study, 32 imprinted genes annotated in public databases were not detected. Fifteen of these did not have SNPs, and most of the remaining 17 genes are known to exhibit imprinting in the placenta only. Thus, known imprinting effects are intact in our data, and we found little evidence for loss of imprinting. Most importantly, we demonstrate that noncanonical imprinting is reproducible in both Cast × B6 and PWD/J × A/J hybrids and occurs in wild-derived, outbred populations. These results provide confidence that our findings are not simply due to disrupted canonical imprinting.

This study refines and substantially extends our early observations on imprinting in the brain (Gregg et al., 2010a; 2010b). Recently, two independent groups published profiles of imprinting in mice, but they disagree in terms of their findings (Babak et al., 2015; Crowley et al., 2015). We identified significant imprinting effects for 22 of the 52 novel genes reported by Crowley et al. at a 1% FDR, and 87% of their novel genes exhibit the same direction of allele bias in our brain data, indicating strong agreement. We did not find evidence for the reported widespread paternal bias on the autosomes (Crowley et al., 2015) but uncovered a significant paternal bias on chromosome 1 in the DRN, and our internal controls indicate that other noncanonical imprinting effects likely remain to be discovered. Finally, we identified imprinting for one of the novel imprinted genes reported by Babak and colleagues (*Edn3*), and our results support their conclusion that imprinting is more prevalent in the brain compared to other tissues (Babak et al., 2015). Our study further reveals that the brain enrichment is largely driven by noncanonical imprinting effects.

EXPERIMENTAL PROCEDURES

Animals

Animal experiments were performed in accordance with protocols approved by the University of Utah Institutional Animal Care and Use Committee. C57BL/6J, CastEiJ, PWD/J, and A/J males and females were obtained from Jackson Laboratory. Idaho wild-derived mice were a gift from Dr. Steven Austad (University of Alabama). *Th* mutant mice were backcrossed onto a B6 background for at least eight generations and were a gift from Dr. Richard Palmiter (University of Washington).

RNA Isolation and RNA-Seq

The ARN, DRN, liver, and thigh muscle were microdissected from female F1 hybrid mice at 8–10 weeks of age. The ARN dissection includes the ventral medial hypothalamus. The DRN dissection includes portions of the ventral periaqueductal gray. The RNA was extracted using the RNAeasy Micro Kit (QIAGEN). RNA was pooled from four to five daughters from different litters to provide ~3 μg of total RNA for each biological replicate. Samples were prepared for RNA-seq using the TruSeq RNA sample preparation kit v2 (RS-122-2001, Illumina). Single-end 59-bp sequencing of the libraries was performed using the Illumina HiSeq 2000.

Allele-Specific ChIP

Chromatin was isolated from the hypothalamus of Cast × B6 F1 hybrid mice and chromatin immunoprecipitation for H3K9ac and H3K9me3 was performed using the Imprint Chromatin Immunoprecipitation kit according to the manufacturer's instructions (CHP1-24RXN, Sigma-Aldrich) and the following antibodies: mouse anti-H3K9ac (ab4441, Abcam) and rabbit anti-H3K9me3 (ab8898, Abcam). Results are normalized to input controls.

mRNA Preparation for Pyrosequencing

Total RNA was purified from the ARN, DRN, liver, or muscle from individual Cast × B6 F1 hybrid offspring using MicroElute Total RNA kit (R6831-02, Omega). The cDNA library was generated using the qScript cDNA supermix (P/N84034, Quanta) and oligo(dT) primers + random hexamer primers according to the manufacturer's instructions.

Pyrosequencing

Pyrosequencing to analyze allele-specific expression effects or allele-specific ChIP for specific genes was performed using the Pyromark System according to manufacturer's instructions (QIAGEN). Amplification primers and sequencing primers are provided in Tables S5 and S7. We performed four to eight biological replicates for each cross and calculated the Cast:B6 allele expression (mRNA) or enrichment (ChIP) ratio for each replicate. Using a one-tailed t test for RNA-seq validation studies and a two-tailed t test for ChIP studies, we compared the Cast:B6 allele expression or enrichment ratio between the F1i and F1r hybrid offspring to test for statistically significant differences between the two crosses.

RNAScope Allele In Situ Hybridization

RNAscope probes targeting specific introns were designed by Advanced Cell Diagnostics (http://www.acdbio.com/), and staining was performed using ACD RNAscope kits according to the manufacturer's instructions on 14-μm

tissue cryosections from female B6 mice. Probes used in this study are available for ordering from ACD.

Behavior Studies

Open-field testing was analyzed by Noldus Ethovision software (http://www.noldus.com/). Sucrose intake was determined for each concentration from 2 days of testing during the light phase with alternate cage bottle positions on each day.

ACCESSION NUMBERS

The RNA-seq data reported in this paper have been deposited to the NCBI GEO and are available under accession number GEO: GSE70484.

SUPPLEMENTAL INFORMATION

Supplemental Information includes Supplemental Results, Supplemental Experimental Procedures, seven figures, and seven tables and can be found with this article online at http://dx.doi.org/10.1016/j.celrep.2015.07.017.

AUTHOR CONTRIBUTIONS

C.G. designed the study and wrote the paper. E.F. and C.G. performed the bioinformatics. W.-C.H. and T.C. performed the pyrosequencing and ChIP studies. W.-C.H. performed the wild-derived mouse experiments. C.G. and C.N.S.H. performed mouse breeding, dissections, sample prep, and data analysis. C.N.S.H., T.C., and P.J.B. performed the RNAscope allele expression studies. P.J.B. performed the behavior and monoamine pathway pyrosequencing studies.

ACKNOWLEDGMENTS

The authors wish to thank Dr. Catherine Dulac for financial support to carry out some of the sequencing performed in this study with funds from The Klarman Foundation for Eating Disorders and Dr. Richard Palmiter for transgenic mice. We thank Dr. Ken Boucher (University of Utah) and Dr. Mark Reimers (Virginia Commonwealth University) for comments and advice on the statistical methods. We wish to thank Drs. Monica Vetter, Jan Christian, Jay Gertz, and Carl Thummel (University of Utah) for critical comments on the manuscript. C.N.S.H. is funded by a Swiss National Science Foundation Postdoctoral Fellowship. P.J.B. is funded by a postdoctoral training award from NIH training grant 5T32DK091317-02. C.G. is a New York Stem Cell Foundation Robertson-Neuroscience Investigator.

Received: December 8, 2014
Revised: June 19, 2015
Accepted: July 8, 2015
Published: July 30, 2015

REFERENCES

Adalsteinsson, B.T., and Ferguson-Smith, A.C. (2014). Epigenetic control of the genome-lessons from genomic imprinting. Genes (Basel) *5*, 635–655.

Babak, T., Deveale, B., Armour, C., Raymond, C., Cleary, M.A., van der Kooy, D., Johnson, J.M., and Lim, L.P. (2008). Global survey of genomic imprinting by transcriptome sequencing. Curr. Biol. *18*, 1735–1741.

Babak, T., DeVeale, B., Tsang, E.K., Zhou, Y., Li, X., Smith, K.S., Kukurba, K.R., Zhang, R., Li, J.B., van der Kooy, D., et al. (2015). Genetic conflict reflected in tissue-specific maps of genomic imprinting in human and mouse. Nat. Genet. *47*, 544–549.

Bahar Halpern, K., Tanami, S., Landen, S., Chapal, M., Szlak, L., Hutzler, A., Nizhberg, A., and Itzkovitz, S. (2015). Bursty gene expression in the intact mammalian liver. Mol. Cell *58*, 147–156.

Bartolomei, M.S., and Ferguson-Smith, A.C. (2011). Mammalian genomic imprinting. Cold Spring Harb. Perspect. Biol. *3*, a002592–a002592.

Calaway, J.D., Lenarcic, A.B., Didion, J.P., Wang, J.R., Searle, J.B., McMillan, L., Valdar, W., and Pardo-Manuel de Villena, F. (2013). Genetic architecture of skewed X inactivation in the laboratory mouse. PLoS Genet. *9*, e1003853.

Carneiro, A.M., Ingram, S.L., Beaulieu, J.-M., Sweeney, A., Amara, S.G., Thomas, S.M., Caron, M.G., and Torres, G.E. (2002). The multiple LIM domain-containing adaptor protein Hic-5 synaptically colocalizes and interacts with the dopamine transporter. J. Neurosci. *22*, 7045–7054.

Chadwick, L.H., and Willard, H.F. (2005). Genetic and parent-of-origin influences on X chromosome choice in Xce heterozygous mice. Mamm. Genome *16*, 691–699.

Challis, C., Boulden, J., Veerakumar, A., Espallergues, J., Vassoler, F.M., Pierce, R.C., Beck, S.G., and Berton, O. (2013). Raphe GABAergic neurons mediate the acquisition of avoidance after social defeat. J. Neurosci. *33*, 13978–13988, 13988a.

Crowley, J.J., Zhabotynsky, V., Sun, W., Huang, S., Pakatci, I.K., Kim, Y., Wang, J.R., Morgan, A.P., Calaway, J.D., Aylor, D.L., et al. (2015). Analyses of allele-specific gene expression in highly divergent mouse crosses identifies pervasive allelic imbalance. Nat. Genet. *47*, 353–360.

Davies, W., Isles, A., Smith, R., Karunadasa, D., Burrmann, D., Humby, T., Ojarikre, O., Biggin, C., Skuse, D., Burgoyne, P., and Wilkinson, L. (2005). Xlr3b is a new imprinted candidate for X-linked parent-of-origin effects on cognitive function in mice. Nat. Genet. *37*, 625–629.

DeVeale, B., van der Kooy, D., and Babak, T. (2012). Critical evaluation of imprinted gene expression by RNA-Seq: a new perspective. PLoS Genet. *8*, e1002600.

Dindot, S.V., Person, R., Strivens, M., Garcia, R., and Beaudet, A.L. (2009). Epigenetic profiling at mouse imprinted gene clusters reveals novel epigenetic and genetic features at differentially methylated regions. Genome Res. *19*, 1374–1383.

Doe, C.M., Relkovic, D., Garfield, A.S., Dalley, J.W., Theobald, D.E.H., Humby, T., Wilkinson, L.S., and Isles, A.R. (2009). Loss of the imprinted snoRNA mbii-52 leads to increased 5htr2c pre-RNA editing and altered 5HT2CR-mediated behaviour. Hum. Mol. Genet. *18*, 2140–2148.

Dölen, G., Darvishzadeh, A., Huang, K.W., and Malenka, R.C. (2013). Social reward requires coordinated activity of nucleus accumbens oxytocin and serotonin. Nature *501*, 179–184.

Fernández-Medarde, A., and Santos, E. (2011). The RasGrf family of mammalian guanine nucleotide exchange factors. Biochim. Biophys. Acta *1815*, 170–188.

Fowlis, D.J., Ansell, J.D., and Micklem, H.S. (1991). Further evidence for the importance of parental source of the Xce allele in X chromosome inactivation. Genet. Res. *58*, 63–65.

Gao, Q., and Horvath, T.L. (2007). Neurobiology of feeding and energy expenditure. Annu. Rev. Neurosci. *30*, 367–398.

Goncalves, A., Leigh-Brown, S., Thybert, D., Stefflova, K., Turro, E., Flicek, P., Brazma, A., Odom, D.T., and Marioni, J.C. (2012). Extensive compensatory cis-trans regulation in the evolution of mouse gene expression. Genome Res. *22*, 2376–2384.

Gregg, C., Zhang, J., Butler, J.E., Haig, D., and Dulac, C. (2010a). Sex-specific parent-of-origin allelic expression in the mouse brain. Science *329*, 682–685.

Gregg, C., Zhang, J., Weissbourd, B., Luo, S., Schroth, G.P., Haig, D., and Dulac, C. (2010b). High-resolution analysis of parent-of-origin allelic expression in the mouse brain. Science *329*, 643–648.

Haig, D. (2000). The kinship theory of genomic imprinting. Annu. Rev. Ecol. Syst. *31*, 9–32.

Huguet, G., Ey, E., and Bourgeron, T. (2013). The genetic landscapes of autism spectrum disorders. Annu. Rev. Genomics Hum. Genet. *14*, 191–213.

Iglesias-Platas, I., Court, F., Camprubi, C., Sparago, A., Guillaumet-Adkins, A., Martin-Trujillo, A., Riccio, A., Moore, G.E., and Monk, D. (2013). Imprinting at the PLAGL1 domain is contained within a 70-kb CTCF/cohesin-mediated non-allelic chromatin loop. Nucleic Acids Res. *41*, 2171–2179.

Ivanova, E., and Kelsey, G. (2011). Imprinted genes and hypothalamic function. J. Mol. Endocrinol. *47*, R67–R74.

Khatib, H. (2007). Is it genomic imprinting or preferential expression? BioEssays *29*, 1022–1028.

Kobayashi, K., Noda, Y., Matsushita, N., Nishii, K., Sawada, H., Nagatsu, T., Nakahara, D., Fukabori, R., Yasoshima, Y., Yamamoto, T., et al. (2000). Modest neuropsychological deficits caused by reduced noradrenaline metabolism in mice heterozygous for a mutated tyrosine hydroxylase gene. J. Neurosci. *20*, 2418–2426.

Korostowski, L., Sedlak, N., and Engel, N. (2012). The Kcnq1ot1 long non-coding RNA affects chromatin conformation and expression of Kcnq1, but does not regulate its imprinting in the developing heart. PLoS Genet. *8*, e1002956.

Lawson, H.A., Cheverud, J.M., and Wolf, J.B. (2013). Genomic imprinting and parent-of-origin effects on complex traits. Nat. Rev. Genet. *14*, 609–617.

Loman, N.J., Misra, R.V., Dallman, T.J., Constantinidou, C., Gharbia, S.E., Wain, J., and Pallen, M.J. (2012). Performance comparison of benchtop high-throughput sequencing platforms. Nat. Biotechnol. *30*, 434–439.

Lowry, C.A., Hale, M.W., Evans, A.K., Heerkens, J., Staub, D.R., Gasser, P.J., and Shekhar, A. (2008). Serotonergic systems, anxiety, and affective disorder: focus on the dorsomedial part of the dorsal raphe nucleus. Ann. N Y Acad. Sci. *1148*, 86–94.

Meacham, F., Boffelli, D., Dhahbi, J., Martin, D.I., Singer, M., and Pachter, L. (2011). Identification and correction of systematic error in high-throughput sequence data. BMC Bioinformatics *12*, 451.

Michelsen, K.A., Schmitz, C., and Steinbusch, H.W.M. (2007). The dorsal raphe nucleus–from silver stainings to a role in depression. Brain Res. Brain Res. Rev. *55*, 329–342.

Miller, R.A., Harper, J.M., Dysko, R.C., Durkee, S.J., and Austad, S.N. (2002). Longer life spans and delayed maturation in wild-derived mice. Exp. Biol. Med. (Maywood) *227*, 500–508.

Monti, J.M. (2010). The structure of the dorsal raphe nucleus and its relevance to the regulation of sleep and wakefulness. Sleep Med. Rev. *14*, 307–317.

Otto, S.P., and Goldstein, D.B. (1992). Recombination and the evolution of diploidy. Genetics *131*, 745–751.

Peters, J. (2014). The role of genomic imprinting in biology and disease: an expanding view. Nat. Rev. Genet. *15*, 517–530.

Prickett, A.R., and Oakey, R.J. (2012). A survey of tissue-specific genomic imprinting in mammals. Mol. Genet. Genomics *287*, 621–630.

Raefski, A.S., and O'Neill, M.J. (2005). Identification of a cluster of X-linked imprinted genes in mice. Nat. Genet. *37*, 620–624.

Schulz, R., Woodfine, K., Menheniott, T.R., Bourc'his, D., Bestor, T., and Oakey, R.J. (2008). WAMIDEX: a web atlas of murine genomic imprinting and differential expression. Epigenetics *3*, 89–96.

Singh, P., Cho, J., Tsai, S.Y., Rivas, G.E., Larson, G.P., and Szabó, P.E. (2010). Coordinated allele-specific histone acetylation at the differentially methylated regions of imprinted genes. Nucleic Acids Res. *38*, 7974–7990.

Sternson, S.M. (2013). Hypothalamic survival circuits: blueprints for purposive behaviors. Neuron *77*, 810–824.

Wang, Q.P., and Nakai, Y. (1994). The dorsal raphe: an important nucleus in pain modulation. Brain Res. Bull. *34*, 575–585.

Wang, X., Sun, Q., McGrath, S.D., Mardis, E.R., Soloway, P.D., and Clark, A.G. (2008). Transcriptome-wide identification of novel imprinted genes in neonatal mouse brain. PLoS ONE *3*, e3839.

Wang, X., Soloway, P.D., and Clark, A.G. (2010). Paternally biased X inactivation in mouse neonatal brain. Genome Biol. *11*, R79.

Wang, X., Soloway, P.D., and Clark, A.G. (2011). A survey for novel imprinted genes in the mouse placenta by mRNA-seq. Genetics *189*, 109–122.

Wang, H., Huang, Z., Huang, L., Niu, S., Rao, X., Xu, J., Kong, H., Yang, J., Yang, C., Wu, D., et al. (2012). Hypothalamic Ahi1 mediates feeding behavior through interaction with 5-HT2C receptor. J. Biol. Chem. *287*, 2237–2246.

Wolf, J.B., Oakey, R.J., and Feil, R. (2014). Imprinted gene expression in hybrids: perturbed mechanisms and evolutionary implications. Heredity (Edinb) *113*, 167–175.

Xie, W., Barr, C.L., Kim, A., Yue, F., Lee, A.Y., Eubanks, J., Dempster, E.L., and Ren, B. (2012). Base-resolution analyses of sequence and parent-of-origin dependent DNA methylation in the mouse genome. Cell *148*, 816–831.

Yang, F., Babak, T., Shendure, J., and Disteche, C.M. (2010). Global survey of escape from X inactivation by RNA-sequencing in mouse. Genome Res. *20*, 614–622.

Zwemer, L.M., Zak, A., Thompson, B.R., Kirby, A., Daly, M.J., Chess, A., and Gimelbrant, A.A. (2012). Autosomal monoallelic expression in the mouse. Genome Biol. *13*, R10.